Front. Optoelectron. 2020, 13(4): 402–408
https://doi.org/10.1007/s12200-019-0960-z

RESEARCH ARTICLE

Time-delay signature characteristics of the chaotic output from an optoelectronic oscillator by introducing an optical feedback

Xixuan LIU, Xi TANG, Zhengmao WU, Guangqiong XIA (✉)

School of Physical Science and Technology, Southwest University, Chongqing 400715, China

Abstract In this work, via autocorrelation function (ACF) and permutation entropy (PE) methods, we numerically investigate the time-delay signature (TDS) characteristics of the chaotic signal output from an optoelectronic oscillator (OEO) after introducing an extra optical feedback loop. The results demonstrate that, for such a chaotic system, both the optoelectronic feedback with a delay time of T_1 and the optical feedback with a delay time of T_2 contribute to the TDS of generated chaos. The TDS of the chaotic signal should be evaluated within a large time window including T_1 and T_2 by the strongest peak in the ACF curve of the chaotic signal, and the strongest peak may locate at near T_1 or T_2. Through mapping the evolution of the TDS in the parameter space of the optical feedback strength and time, certain optimized parameter regions for achieving a chaotic signal with a relatively weak TDS can be determined.

Keywords optoelectronic oscillator (OEO), chaotic output, time-delay signature (TDS), optical feedback

1 Introduction

Chaotic dynamics of optical systems have attracted considerable attention due to their promising applications such as secure optical communication system [1–3], high speed random number generation (RNG) [4–6], optical time domain reflectometer [7,8] and chaotic radar [9–11], etc. Semiconductor lasers are the most popular sources to achieve optical chaos, and the generation ways of optical chaos based on semiconductor lasers can be divided into two categories: one is based on the nonlinear effect of lasers through introducing one or more external perturbations such as optical feedback [12–15], optical injection [16,17] and optoelectronic feedback [18,19], which can be described by Lang-Kobayashi rate equations [20]; the other is based on the nonlinear effect of an external passive nonlinear device, where an optoelectronic oscillator (OEO) [21–24] is a typical device and can be described by Ikeda's delay differential equations [25]. For traditional OEO-based chaotic systems, the chaos can be generated by that a continuous wave (CW) light output from a laser goes through an optoelectronic feedback loop, in which a passively nonlinear optical device is contained. It is worth noting that the laser is treated as a linear light source operating at a stable state [26]. Usually, time-delay signature (TDS) inevitably exists in the chaotic output of a traditional OEO due to optoelectronic feedback loop. Generally, taking a chaotic signal with obvious TDS as a chaotic carrier, the security of the chaotic secure communication will be reduced [27]. Taking a chaotic signal with obvious TDS for high speed RNG, the randomness property of RNG will be degraded due to the recurrence features induced by the TDS [28]. As a result, some effective schemes have been proposed in succession to reduce (or suppress) the TDS of the chaotic output from OEO-based chaotic systems. For example, instead of a CW by a chaotic signal output from an optical feedback laser, the TDS in the OEO-based chaotic system is successfully hidden [29]. By adopting multiple electro-optic nonlinear loops, the TDS can also be effectively suppressed [30]. Based on a two-dimensional coupled optoelectronic delay feedback system with variable parameters, an obvious reduction of the TDS can be accomplished [31].

Recently, a simple and easily implemented scheme is proposed to reduce the TDS in an OEO-based chaotic system [32]. For this scheme, an extra optical feedback loop with a delay time of T_2 is introduced into an OEO-based chaotic system. The TDS of the chaotic output is

Received August 10, 2019; accepted September 23, 2019

E-mail: gqxia@swu.edu.cn

analyzed in a vicinity of the optoelectronic feedback time T_1, and the results demonstrate that the TDS can be effectively suppressed. However, as is well known, an extra optical feedback loop will lead to another TDS located near T_2, and the TDS should be inspected simultaneously at the vicinities of T_1 and T_2. As a result, in this work, within a large time window including T_1 and T_2, the TDS of the chaotic signal from an OEO after introducing an extra optical feedback loop is analyzed, and some optimized parameters for generating a chaotic signal with reduced TDS have been specified.

2 System model and theory

Figure 1 is a schematic diagram for a chaotic signal generation based on an OEO after introducing an extra optical feedback. A laser diode is used to generate a CW light, which is sent to a Mach-Zehnder modulator (MZM) with a radio frequency (RF) half-wave voltage of $V_{\pi RF}$ after passing through a polarization controller 1 to match the polarization of the CW light with that of the MZM. The MZM output is divided into two parts by an optical fiber coupler 2. One passes through a delay line 1 and is converted into an electrical signal by a photodetector (PD). The electrical signal is further amplified by a radio frequency amplifier (RFA), and the amplifier also plays a role of a band-pass filter with a low cut-off frequency of f_L and a high cut-off frequency of f_H. Finally, the amplified electrical signal $V(t)$ depended on the conversion efficiency of PD and the magnification of RFA, is sent into the MZM and constitutes an optoelectronic feedback loop with a delay time of T_1. The other part is injected into an optical feedback loop composed by a delay line 2, a variable attenuator, a polarization controller 2, a fiber coupler 1 and a polarization controller 1, and the delay time of the feedback loop is T_2. The variable attenuator is employed to control the optical feedback strength K, and the polarization controller 2 is utilized to match the polarization of the optical feedback with that of MZM for maximizing the coupling efficiency.

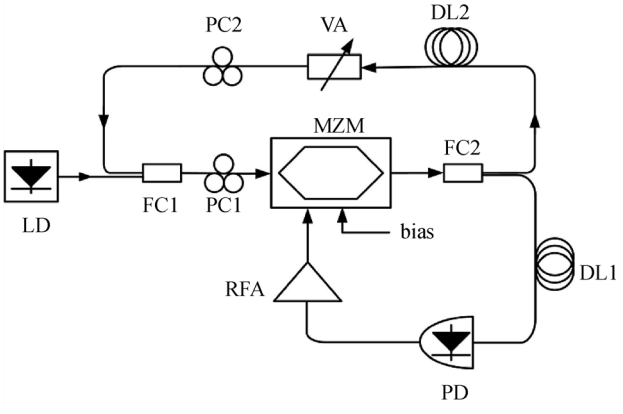

Fig. 1 Schematic diagram of a chaotic signal generation based on an OEO after introducing an extra optical feedback. LD: laser diode; FC: fiber coupler; PC: polarization controller; MZM: Mach-Zehnder modulator; DL: delay line; PD: photodetector; RFA: radio frequency amplifier; VA: variable attenuator

Based on the Ikeda rate equations [25] and taking an extra optical feedback into account, for convenient for comparing with the results obtained in Ref. [32], the dynamical equations of the chaotic system mentioned above can be described by [32]

$$\frac{dx(t)}{dt} = -\frac{1}{t_H}\left\{x(t) + \frac{1}{t_L}y(t) - P_{in}(t-T_1) \times Q \times \cos^2[x(t-T_1) + \phi]\right\}, \quad (1)$$

$$P_{in}(t) = P_0 + K \times P_{in}(t-T_2) \times \cos^2[x(t-T_2) + \phi], \quad (2)$$

$$\frac{dy(t)}{dt} = x(t), \quad (3)$$

where $x(t) = \pi V(t)/(2V_{\pi RF})$, $t_H = 1/(2\pi f_H)$, $t_L = 1/(2\pi f_L)$, and $Q = \pi gAG/(2V_{\pi RF})$ (A represents the total attenuation of the optoelectronic feedback loop, g and G are the conversion efficiency of PD and the gain of RFA, respectively). P_0 is the laser output power, and $P_{in}(t)$ is the coupled input power of MZM. P_0Q represents the strength of the nonlinear function, which plays an important role in the chaotic behavior with high complexity.

Some methods such as autocorrelation function (ACF), delay mutual information method [33], permutation entropy (PE) [34,35], sample entropy [36] and Kolmogorov-Sinai entropy [37] can be used to qualitatively evaluate the TDS, where each approach possesses its unique virtues and respective limitations. In this work, we adopt both ACF and PE methods. For a delay-differential system, ACF is defined as follow:

$$ACF(\Delta t) = \frac{\langle [x(t) - \langle x(t)\rangle][x(t+\Delta t) - \langle x(t)\rangle]\rangle}{\sqrt{\langle (x(t) - \langle x(t)\rangle)^2\rangle \langle (x(t+\Delta t) - \langle x(t)\rangle)^2\rangle}}, \quad (4)$$

where Δt indicates the time shift, $\langle\cdot\rangle$ denotes the time average, and $x(t)$ stands for chaotic time series. We set $\Delta t \in$ [0 ns, 40 ns] and the time series length is taken as 10 μs during calculating ACF.

The PE method, which is based on information theory, has some unique advantages such as simplicity, extremely fast calculation, robustness to noise and easily estimation for any type of time series [34,35,37], and can be defined as follows: an arbitrary time series $X = \{x(t), t = 1,2,\ldots, T\}$ is first reconstructed into a set of D-dimensional vectors after choosing an appropriate embedding dimension D and embedding delay time τ. Then we study all $D!$ permutation π of order D. For each π, the relative frequency is

determined as

$$p(\pi) = \frac{\#\{t|t \leqslant T-D,\ X \text{ has type } \pi\}}{T-D+1}, \tag{5}$$

where # notes number. Hence, PE is defined as

$$h(P) = -\Sigma p(\pi)\log p(\pi), \tag{6}$$

where $P = \{p(\pi)\}$ stands for probability distribution. The normalized PE can be further expressed as

$$H(P) = \frac{h(P)}{h_{\max}} = \frac{-\Sigma p(\pi)\log p(\pi)}{\log(D!)}, \tag{7}$$

where the value of $H(P)$ ranges from 0 to 1. $H(P) = 0$ means that the time series is predictable and regular while $H(P) = 1$ corresponds to a completely stochastic process. After considering the suggestion in Ref. [34], D is fixed at 6 and the time series length is set as 10 μs for the calculation of PE.

3 Results and discussion

Equations (1)–(3) can be numerically solved by adopting fourth-order Runge-Kutta algorithm with a step of 5 ps via MATLAB software. During the calculations, the parameters are chosen as [32]: t_H= 25 ps, t_L= 5 μs, $\phi = -\pi/4$. Unless otherwise specified, Q and P_0 take 1000 W^{-1} and 5 mW, respectively, i.e., $P_0Q = 5$, which can be attained in practical systems [38,39].

First, for T_1 = 30 ns and T_2 = 25 ns, the output characteristics of the OEO subject to optical feedback with different feedback strength K are investigated. Figure 2 displays the time series (a), power spectra (b), zoom-in power spectra (c), ACF curves (d) and PE curves (e) of the chaotic output for K = 0 (first row), 0.2 (second row), 0.5 (third row) and 0.8 (fourth row), respectively. As shown in Figs. 2(a1)–2(a4), the evolutions of the time series are complex, from which it is hard to directly observe a TDS. However, the TDS can be extracted from the power spectra, ACF and PE curves. For K = 0 (first row), there are some equidistant peaks emerging in the power spectrum, and the frequency interval is about 33.3 MHz which is equal to a reciprocal of the optoelectronic feedback delay time T_1. Correspondingly, an obvious peak (0.62) located at T_1 can be observed in Fig. 2(d1), and meanwhile some obvious downward peaks located at T_1 and the subharmonics of T_1 can be found in Fig. 2(e1). As demonstrated in Ref. [35], when an embedding delay matches harmonics and subharmonics of the feedback time, PE will arrive at its minima and emergences a downward peak. For an embedding dimension D, there are D-2 subharmonics peaks. Since we set D = 6 and T_1 = 30 ns, there are four subharmonic peaks located at 15, 10, 7.5, and 6 ns, respectively. Under this case, TDS is only determined by the optoelectronic feedback. For K = 0.2 (second row), the frequency intervals between two adjacent peaks in power spectrum are not the same, and a new peak originating from optical feedback appears at the optical feedback time T_2 in the ACF curve. Meantime, some extra sharp downward peaks can be observed in PE curve at T_2 and its integer fractions. Under this circumstance, TDS should

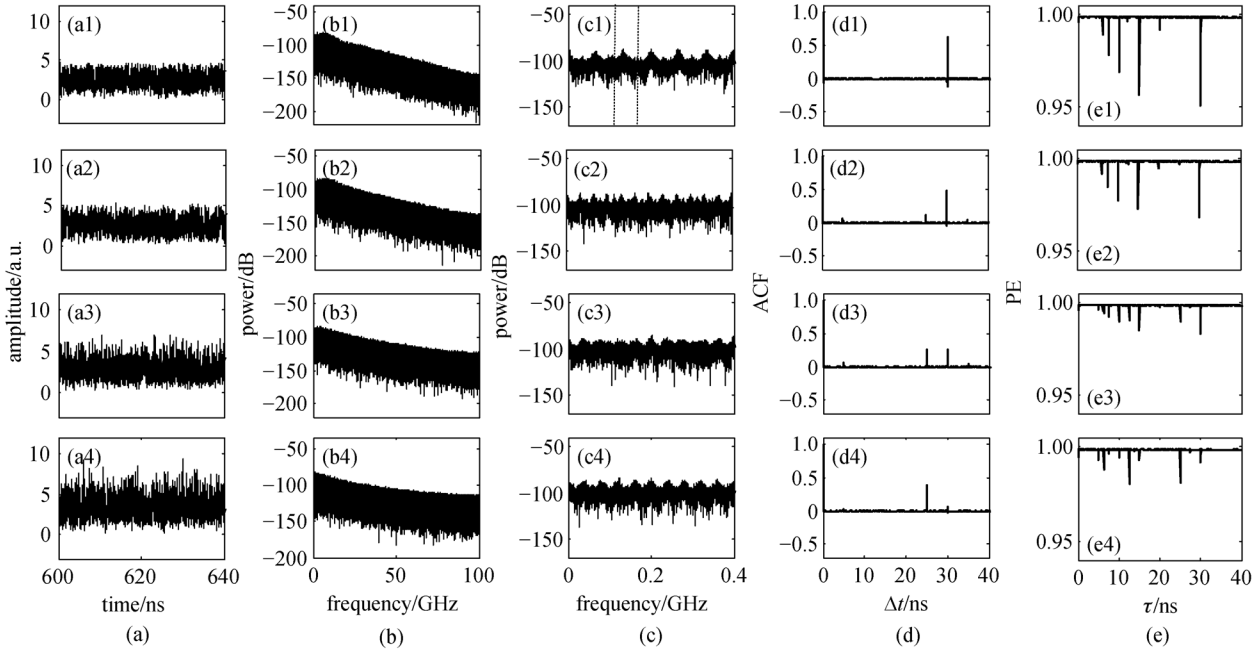

Fig. 2 (a) Time series, (b) power spectra, (c) zoom-in power spectra, (d) ACF curves and (e) PE curves of the chaotic signal from an OEO after introducing an extra optical feedback with T_1 = 30 ns and T_2 = 25 ns, where the first, second, third and fourth rows represent an optical feedback strength K of 0, 0.2, 0.5 and 0.8, respectively

be quantified by the strongest peak (0.48) in ACF curve or the deepest downward peak in PE curve. Obviously, the TDS is still determined by optoelectronic feedback, which is weaker than that for $K = 0$. The reason for the weakening of TDS may be due to the complexity improvement originating from the introduction of optical feedback [32]. For $K = 0.5$ (third row), the power spectrum becomes much smoother and no significant peaks appears, then the TDS cannot be identified from the power spectrum due to the joint action of optical feedback and optoelectronic feedback. However, from Figs. 2(d3) and 2(e3), it can be seen that the amplitude of the peak (downward peak) locating at T_1 is similar with that locating at T_2 in ACF curve (PE curve). As a result, the optical feedback devotes the same degree TDS as that for the optoelectronic feedback, and the maximum of ACF is about 0.26. In particular, for $K = 0.8$, the TDS resulted by optoelectronic feedback is greatly reduced, but the TDS is still very obvious (as shown in Figs. 2(d4) and 2(e4)) due to the recurrence feature induced by the strong optical feedback strength. Meanwhile, some peaks with an equal frequency interval emerge in the power spectrum, and the frequency interval is equal to a reciprocal of T_2. Under this case, the TDS is mainly originated from the optical feedback. Therefore, for an OEO subject to an extra optical feedback, the TDS of the generated chaotic signal should be inspected not only at the vicinity of T_1 but also at the vicinity of T_2.

Since PE curves exhibit similar properties with ACF curves, we adopt the ACF method in the following discussion. Figure 3(a) shows the maps of ACF curves for $T_1 = 30$ ns and $T_2 = 25$ ns with K varied from 0 to 1, and Figs. 3(b) and 3(c) is the correspondingly expanded version at the vicinity of T_2 and T_1, respectively. Obviously, with the increase of K, the TDS at T_2 gradually enhances while the TDS at T_1 gradually weakens. In other words, the dominant role for contributing TDS undergoes a switch from optoelectronic feedback to optical feedback during increasing K. Under the other parameters given above, there exists an optimal K (named as K_{optimal}), under

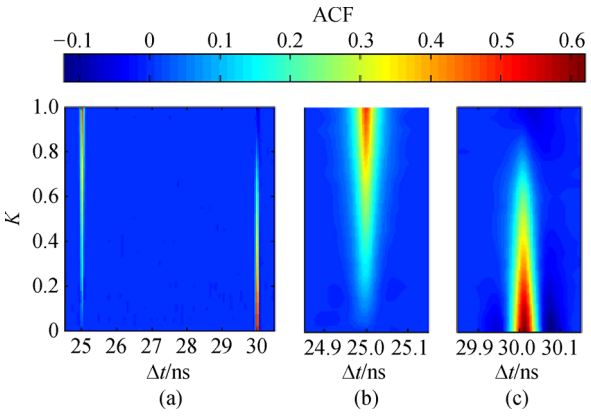

Fig. 3 (a) Calculated map of ACF curves for $T_1 = 30$ ns and $T_2 = 25$ ns with K varied from 0 to 1 and the expanded versions of the ACF curve at the vicinities of (b) T_2 and (c) T_1, respectively

which the ACF peak within a large time window including T_1 and T_2 is the weakest.

Next, to find the K_{optimal} value, we calculate the maximum value (σ) of ACF within a large time window including T_1 and T_2 under different K, which is shown in Fig. 4(a). Under $P_0 = 5$ mW, with the increase of K, σ first decreases, after passing through a minimum of 0.26, and then increases. K_{optimal} is about 0.55 and the minimum of σ (named as σ_{min}) is 0.26 for $P_0 = 5$ mW. For P_0 taking different values between 4 to 10 mW (corresponding to different P_0Q values between 4 to 10), the calculated results are presented in Fig. 4(b). It can be observed that both K_{optimal} and σ_{min} show monotonously downward trends with the increase of P_0, and σ_{min} arrives at about 0.04 for $P_0 = 10$ mW. As a result, a relatively large P_0 is helpful for effectively reducing TDS.

Since the above results are obtained under a fixed $T_2 = 25$ ns, we further analyze the evolution of the TDS under different T_2. Figure 5 displays a calculated map of σ in the parameter space of T_2 and K under $T_1 = 30$ ns. From this diagram, it can be seen that the TDS cannot be efficiently

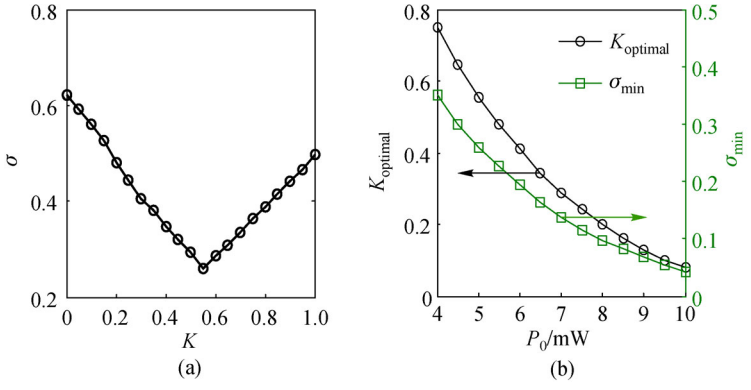

Fig. 4 (a) Dependence of σ on the optical feedback strength K under $P_0 = 5$ mW; (b) dependence of K_{optimal} on the laser power P_0 and corresponding σ_{min} under fixed P_0 and K_{optimal}

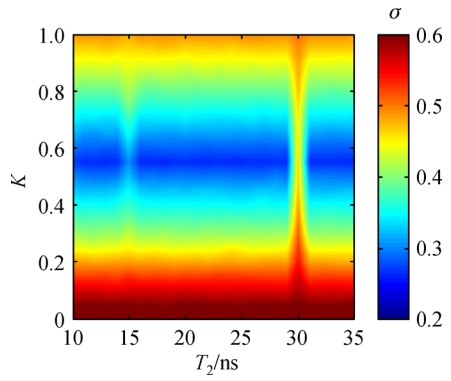

Fig. 5 Calculated map of σ in the parameter space of T_2 and K under T_1 = 30 ns

reduced for too small or too large K. As pointed out in Ref. [13], for a chaotic system with two feedback loops, the TDS of the chaotic output is formed due to a joint action of the two feedback loops, and meanwhile the intrinsic characteristic time of the oscillator takes an important role for the TDS reduction/suppression. For a too small (or too large) K, the TDS is mainly depended on the optoelectronic feedback (or optical feedback) loop, and the joint action of the optical feedback and optoelectronic feedback is less effective. On the contrary, as shown in this diagram, for $K \in [0.4, 0.7]$, the TDS can be effectively reduced except that T_2 is located at the vicinity of 30 ns or 15 ns.

The result in Fig. 5 shows that the value of T_2 seriously affects the TDS of the chaotic output. Finally, we calculate σ in the parameter space of T_1 and T_2 under K = 0.55 in Fig. 6. Obviously, for the relationship of T_2 and T_1 is close to an integral multiple, the TDS of the chaotic signal is enhanced. Especially, under the case of $T_2 = T_1$, the TDS distinctly strengthens, which is easy to understand as follows. Under this case, the location of TDS originating from optical feedback is the same as that from optoelectronic feedback, and then the introduction of an extra optical feedback will further enhance the chaotic TDS. Therefore, the optical feedback time T_2 should be deviated from T_1 and its integer fractions in practice.

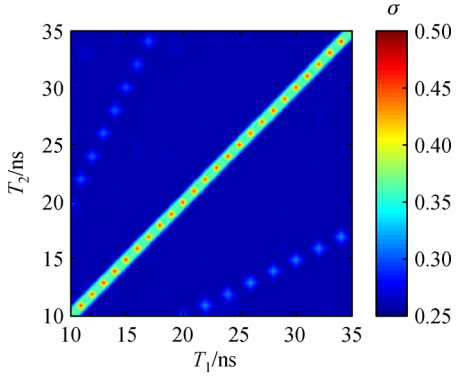

Fig. 6 Calculated map of σ in the parameter space of T_1 and T_2 under K = 0.55

4 Conclusions

In summary, the TDS of the chaotic signal output from an OEO subject to an extra optical feedback is numerically investigated via ACF and PE methods. The simulated results show that, with the increase of the optical feedback strength, the TDS at T_1 originating from the optoelectronic feedback is weakened, but an extra TDS emerging at the vicinity of the optical feedback time T_2 is strengthened. Therefore, the TDS of this chaotic system should be evaluated by the joint action of both the optoelectronic and optical feedback loops. Through adopting the strongest peak value (σ) of ACF curve within a large time window including T_1 and T_2 to characterize the TDS of the chaotic signal, the TDS evolution in the parameter space of K and T_2 has been calculated. The results show that, under a laser power of P_0 = 5 mW, the TDS can be effectively reduced for an optical feedback strength of $K \in [0.4, 0.7]$ and T_2 deviated from T_1 and its integer fractions. Additionally, a larger P_0 is helpful for achieving a chaotic signal with lower TDS.

Acknowledgements This work was supported by the National Natural Science Foundation of China (Grant Nos. 61575163, 61775184, 11704316, and 61875167).

References

1. Argyris A, Syvridis D, Larger L, Annovazzi-Lodi V, Colet P, Fischer I, García-Ojalvo J, Mirasso C R, Pesquera L, Shore K A. Chaos-based communications at high bit rates using commercial fibre-optic links. Nature, 2005, 438(7066): 343–346
2. Hong Y H, Lee M W, Paul J, Spencer P S, Shore K A. GHz bandwidth message transmission using chaotic vertical-cavity surface-emitting lasers. Journal of Lightwave Technology, 2009, 27(22): 5099–5105
3. Chiarello F, Ursini L, Santagiustina M. Securing wireless infrared communications through optical chaos. IEEE Photonics Technology Letters, 2011, 23(9): 564–566
4. Uchida A, Amano K, Inoue M, Hirano K, Naito S, Someya H, Oowada I, Kurashige T, Shiki M, Yoshimori S, Yoshimura K, Davis P. Fast physical random bit generation with chaotic semiconductor lasers. Nature Photonics, 2008, 2(12): 728–732
5. Kanter I, Aviad Y, Reidler I, Cohen E, Rosenbluh M. An optical ultrafast random bit generator. Nature Photonics, 2010, 4(1): 58–61
6. Sakuraba R, Iwakawa K, Kanno K, Uchida A. Tb/s physical random bit generation with bandwidth-enhanced chaos in three-cascaded semiconductor lasers. Optics Express, 2015, 23(2): 1470–1490
7. Wang Y C, Wang B J, Wang A B. Chaotic correlation optical time domain reflectometer utilizing laser diode. IEEE Photonics Technology Letters, 2008, 20(19): 1636–1638
8. Wang A B, Wang N, Yang Y B, Wang B J, Zhang M J, Wang Y C. Precise fault location in WDM-PON by utilizing wavelength tunable chaotic laser. Journal of Lightwave Technology, 2012, 30(21): 3420–3426

9. Lin F Y, Liu J M. Chaotic radar using nonlinear laser dynamics. IEEE Journal of Quantum Electronics, 2004, 40(6): 815–820
10. Lin F Y, Liu J M. Chaotic lidar. IEEE Journal of Selected Topics in Quantum Electronics, 2004, 10(5): 991–997
11. Wu W T, Liao Y H, Lin F Y. Noise suppressions in synchronized chaos lidars. Optics Express, 2010, 18(25): 26155–26162
12. Rontani D, Locquet A, Sciamanna M, Citrin D S, Ortin S. Time-delay identification in a chaotic semiconductor laser with optical feedback: a dynamical point of view. IEEE Journal of Quantum Electronics, 2009, 45(7): 879–891
13. Wu J G, Xia G Q, Wu Z M. Suppression of time delay signatures of chaotic output in a semiconductor laser with double optical feedback. Optics Express, 2009, 17(22): 20124–20133
14. Zhang L, Pan B, Chen G, Guo L, Lu D, Zhao L, Wang W. 640-Gbit/s fast physical random number generation using a broadband chaotic semiconductor laser. Scientific Reports, 2017, 7(1): 45900
15. Masoller C. Anticipation in the synchronization of chaotic semiconductor lasers with optical feedback. Physical Review Letters, 2001, 86(13): 2782–2785
16. Zhong D, Yang G, Xiao Z, Ding Y, Xi J, Zeng N, Yang H. Optical chaotic data-selection logic operation with the fast response for picosecond magnitude. Optics Express, 2019, 27(16): 23357–23367
17. Chen J J, Duan Y N, Li L F, Zhong Z Q. Wideband polarization-resolved chaos with time-delay signature suppression in VCSELs subject to dual chaotic optical injections. IEEE Access: Practical Innovations, Open Solutions, 2018, 6: 66807–66815
18. Abarbanel H D I, Kennel M B, Illing L, Tang S, Chen H F, Liu J M. Synchronization and communication using semiconductor lasers with optoelectronic feedback. IEEE Journal of Quantum Electronics, 2001, 37(10): 1301–1311
19. Liao J F, Sun J Q. Polarization dynamics and chaotic synchronization in unidirectionally coupled VCSELs subjected to optoelectronic feedback. Optics Communications, 2013, 295: 188–196
20. Lang R, Kobayashi K. External optical feedback effects on semiconductor injection laser properties. IEEE Journal of Quantum Electronics, 1980, 16(3): 347–355
21. Larger L, Lee M W, Goedgebuer J P, Elflein W, Erneux T. Chaos in coherence modulation: bifurcations of an oscillator generating optical delay fluctuations. Journal of the Optical Society of America B, Optical Physics, 2001, 18(8): 1063–1068
22. Larger L, Dudley J M. Optoelectronic chaos. Nature, 2010, 465 (7294): 41–42
23. Kouomou Y C, Colet P, Larger L, Gastaud N. Chaotic breathers in delayed electro-optical systems. Physical Review Letters, 2005, 95 (20): 203903
24. Callan K E, Illing L, Gao Z, Gauthier D J, Schöll E. Broadband chaos generated by an optoelectronic oscillator. Physical Review Letters, 2010, 104(11): 113901
25. Ikeda K, Matsumoto K. High-dimensional chaotic behavior in systems with time-delayed feedback. Physica D, Nonlinear Phenomena, 1987, 29(1–2): 223–235
26. Murphy T E, Cohen A B, Ravoori B, Schmitt K R B, Setty A V, Sorrentino F, Williams C R S, Ott E, Roy R. Complex dynamics and synchronization of delayed-feedback nonlinear oscillators. Philosophical Transactions of Royal Society A, 2010, 368(1911): 343–366
27. Prokhorov M D, Ponomarenko V I, Karavaev A S, Bezruchko B P. Reconstruction of time-delayed feedback systems from time series. Physica D. Nonlinear Phenomena, 2005, 203(3–4): 209–223
28. Tang X, Wu Z M, Wu J G, Deng T, Chen J J, Fan L, Zhong Z Q, Xia G Q. Tbits/s physical random bit generation based on mutually coupled semiconductor laser chaotic entropy source. Optics Express, 2015, 23(26): 33130–33141
29. Hizanidis J, Deligiannidis S, Bogris A, Syvridis D. Enhancement of chaos encryption potential by combining all-optical and electro-optical chaos generators. IEEE Journal of Quantum Electronics, 2010, 46(11): 1642–1649
30. Gao X, Cheng M, Deng L, Liu L, Hu H, Liu D. A novel chaotic system with suppressed time-delay signature based on multiple electro-optic nonlinear loops. Nonlinear Dynamics, 2015, 82(1–2): 611–617
31. Liu L F, Miao S X, Cheng M F, Gao X J. Two-dimensional coupled electro-optic delayed feedback system with varying parameters. Journal of Modern Optics, 2017, 64(6): 547–554
32. Hu H P, Shi S Y, Xie F L. Electro-optic intensity chaotic system with an extra optical feedback. Optics Communications, 2017, 402: 140–146
33. Rontani D, Locquet A, Sciamanna M, Citrin D S. Loss of time-delay signature in the chaotic output of a semiconductor laser with optical feedback. Optics Letters, 2007, 32(20): 2960–2962
34. Bandt C, Pompe B. Permutation entropy: a natural complexity measure for time series. Physical Review Letters, 2002, 88(17): 174102
35. Soriano M C, Zunino L, Rosso O A, Fischer I, Mirasso C R. Time scales of a chaotic semiconductor laser with optical feedback under the lens of a permutation information analysis. IEEE Journal of Quantum Electronics, 2011, 47(2): 252–261
36. Li N, Pan W, Xiang S, Zhao Q, Zhang L, Mu P. Quantifying the complexity of the chaotic intensity of an external-cavity semiconductor laser via sample entropy. IEEE Journal of Quantum Electronics, 2014, 50(9): 766–773
37. Zunino L, Rosso O A, Soriano M C. Characterizing the hyperchaotic dynamics of a semiconductor laser subject to optical feedback via permutation entropy. IEEE Journal of Selected Topics in Quantum Electronics, 2011, 17(5): 1250–1257
38. Lavrov R, Peil M, Jacquot M, Larger L, Udaltsov V, Dudley J. Electro-optic delay oscillator with nonlocal nonlinearity: Optical phase dynamics, chaos, and synchronization. Physical Review. E, 2009, 80(2): 026207
39. Lavrov R, Jacquot M, Larger L. Nonlocal nonlinear electro-optic Phase dynamics demonstrating 10 Gbs/s chaos communications. IEEE Journal of Quantum Electronics, 2010, 46(10): 1430–1435

Xixuan Liu received the B.S. degree in electronic and information engineering from Shandong Normal University, Jinan, China, in 2017. She is currently working toward her M.Sc. degree in signal and information processing at the Southwest University. Her main research focuses on the nonlinear dynamics and chaos of semiconductor lasers.

Xi Tang received the M.Sc. degree in optics from Southwest University, Chong qing, China, in 2009. He is currently working toward the Ph.D. degree in optics at the Southwest University. He has co-authored over 20 publications. His research direction mainly focuses on random number generation based on chaotic semiconductor lasers.

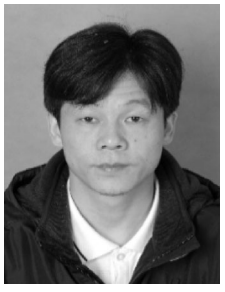

Zhengmao Wu received the B.Sc., M.Sc. and Ph.D. degrees in optics from Sichuan University, Chengdu, Sichuan, China, in 1992, 1995 and 2003, respectively. At present, he is a full Professor with the School of Physical Science and Technology, Southwest University, Chongqing, China. He has authored or co-authored over 150 journal publications. His current research interests include the nonlinear dynamics of semiconductor lasers and their applications, chaotic semiconductor lasers and their applications, photonic reservoir computing.

Guangqiong Xia received the B.Sc., M.Sc. and Ph.D. degrees in optics from Sichuan University, Chengdu, Sichuan, China, in 1992, 1995 and 2002, respectively. At present, she is a full Professor with the School of Physical Science and Technology, Southwest University, Chongqing, China. She has authored or co-authored over 160 journal publications. Her current research interests include the nonlinear dynamics of semiconductor lasers, synchronization and control of chaotic semiconductor lasers, chaos secure communication based on semiconductor lasers, microwave photonics, and photonic reservoir computing and its applications.